Critical moisture point of sludge and its link to vapour sorption and dewatering

Nielsen, Rikke Vilsøe; Jensen, Michelle; Duus, Silas Alf Christian; Christensen, Morten Lykkegaard

Published in:
Chemosphere

DOI (link to publication from Publisher):
10.1016/j.chemosphere.2019.07.030

Publication date:
2019

Document Version
Accepted author manuscript, peer reviewed version

Accepted Manuscript

Critical moisture point of sludge and its link to vapour sorption and dewatering

Rikke Vilsøe Nielsen, Michelle Jensen, Silas Alf Christian Duus, Morten Lykkegaard Christensen

PII: S0045-6535(19)31510-3

DOI: https://doi.org/10.1016/j.chemosphere.2019.07.030

Reference: CHEM 24299

To appear in: *ECSN*

Received Date: 1 April 2019

Revised Date: 7 June 2019

Accepted Date: 4 July 2019

Please cite this article as: Nielsen, Rikke.Vilsø., Jensen, M., Christian Duus, S.A., Christensen, M.L., Critical moisture point of sludge and its link to vapour sorption and dewatering, *Chemosphere* (2019), doi: https://doi.org/10.1016/j.chemosphere.2019.07.030.

Critical moisture point of sludge and its link to vapour sorption and dewatering

Rikke Vilsøe Nielsen, Michelle Jensen, Silas Alf Christian Duus, Morten Lykkegaard Christensen*

Department of Chemistry and Bioscience, Aalborg University, Fredrik Bajers Vej 7H, DK-9220, Aalborg Øst, Denmark

* Corresponding author. Tel.: +45 9940 8464; Fax: +45 9635 0558; E-mail address: mlc@bio.aau.dk (M.L. Christensen).

Abstract

The mechanical dewatering of sludge is important in order to achieve a high dry matter content, thereby lowering the transportation cost and the energy consumption during incineration. Thermogravimetric analysis is sometimes used to estimate the maximum dry matter content obtainable from mechanical dewatering, by measuring the critical moisture point. In this paper, the critical moisture point of digested sludge was measured and compared with vapour sorption curves. The critical moisture point was determined for raw and conditioned sludge to be 3.4 kg of water per kg of dry matter, corresponding to 23% w/w dry matter. This value was lower than the dry matter content obtained from the mechanical dewatering process, indicating that the dry matter content can exceed the critical moisture point. Moisture vapour sorption was measured for raw, conditioned, and dewatered sludges. The Blahovec and Yanniotis sorption isotherm fitted the experimental data well. Between 10 and 12 g of water was adsorbed as a monolayer per 100 g of dry matter. The rest of the moisture content was explained by the non-ideal Raoult's law, by including the effect of dissolved ions. At water activities above 0.95, the moisture content was determined by capillary condensation and cake compressibility. The water activity was higher than 0.95 at the critical moisture point and the capillary pressure was estimated to be 4–6 bars. This pressure was responsible for cake compression

during drying, while the relatively low dry matter content at the critical moisture point may be due to the low capillary pressure.

Keywords: Drying; Critical moisture point; Filtration; Thermogravimetric analysis; Wastewater

1. Introduction

Mechanical dewatering, for example, by filtration and centrifugation, is used to increase the dry matter content of biological sludge, thereby lowering the transportation cost and the energy consumption during incineration. Sludge composition, pretreatment, and settings for the dewatering process all affect the finale dry matter content. It is therefore difficult to find out whether the low dry matter content of dewatered sludge is caused by changes in sludge composition or by problems with pretreatment and dewatering. To solve this problem, Kopp et al. (1–3) developed a thermogravimetric method to predict the maximum dry matter content obtainable by mechanically dewatering a given type of sludge: the sludge is dried, and the critical moisture point is determined and then used as an estimate of the maximum dry matter content (1).

The drying process, as illustrated in Fig. 1, comprises three periods: the initial period, the constant rate period, and the falling rate period (4,5). During the initial period (period A), the weight loss of the cake is low and the capillary pressure increases. The cake starts to shrink when the capillary pressure exceeds the strength of the cake structure and the drying process enters period B, when the drying rate is constant if the external conditions (i.e., air temperature, moisture content, and velocity) remain constant and crust formation is avoided (6,7). The process continues until the compressive strength of the cake structure is high enough to withstand the capillary pressure, after which the drying rate starts to decrease and the drying process enters the falling rate period (period C). The moisture content at the transition between the constant and falling rate periods is called the critical moisture point. At this point, the cake structure is strong enough to withstand the capillary pressure and the pores at the top of the cake dry out; shortly after the critical moisture point is

48 reached, the cake stops shrinking (8). The critical moisture point is therefore determined from the capillary
49 pressure and the strength of the cake structure (Fig. 2). The critical moisture point is reached when the radius
50 of the meniscus equals the radius of the pores in the cakes. The capillary pressure and cake compression
51 thereby depend on the pore size in the cake structure.

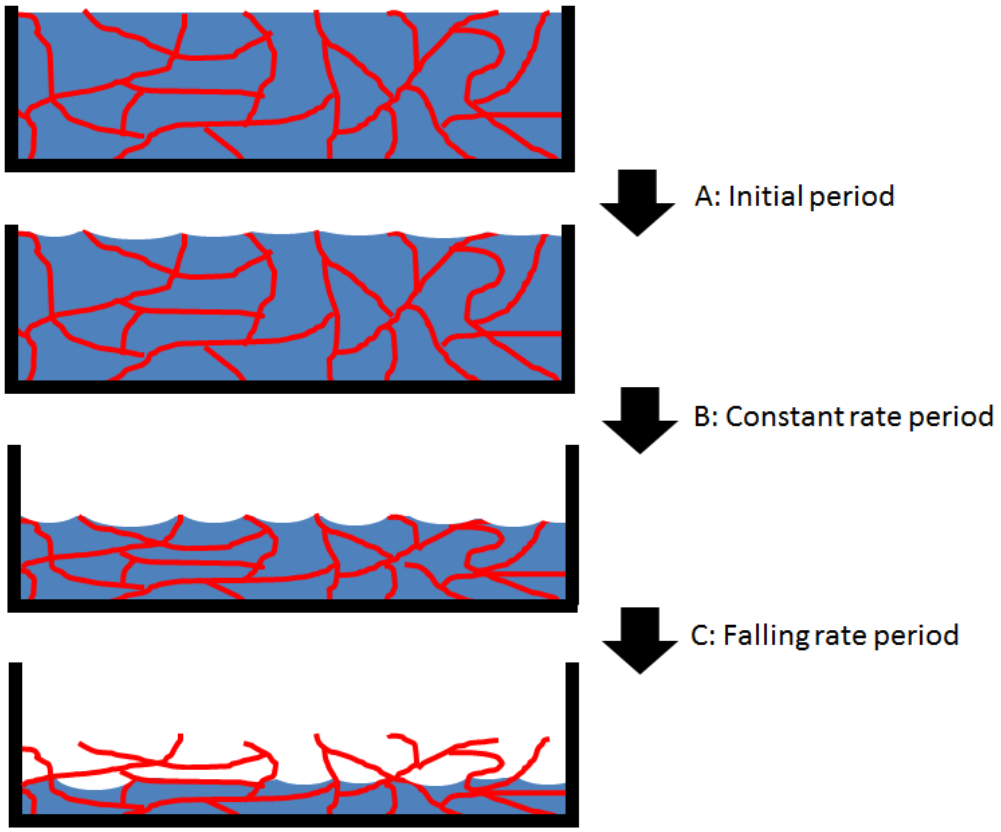

52

53 **Fig. 1.** Schematic of the drying process.

54 The falling rate period (period C) can be divided into two: the first and second falling rate periods (4).
55 During the first falling rate period, the meniscus retreats into the cake structure, but there is a continuous
56 layer of liquid on the pore walls, so liquid flow from the inner cake structure to the surface is still possible. In
57 the secondary falling rate period, the liquid cannot flow on the pore walls and the liquid transport in the
58 pores is mainly due to vapour diffusion.

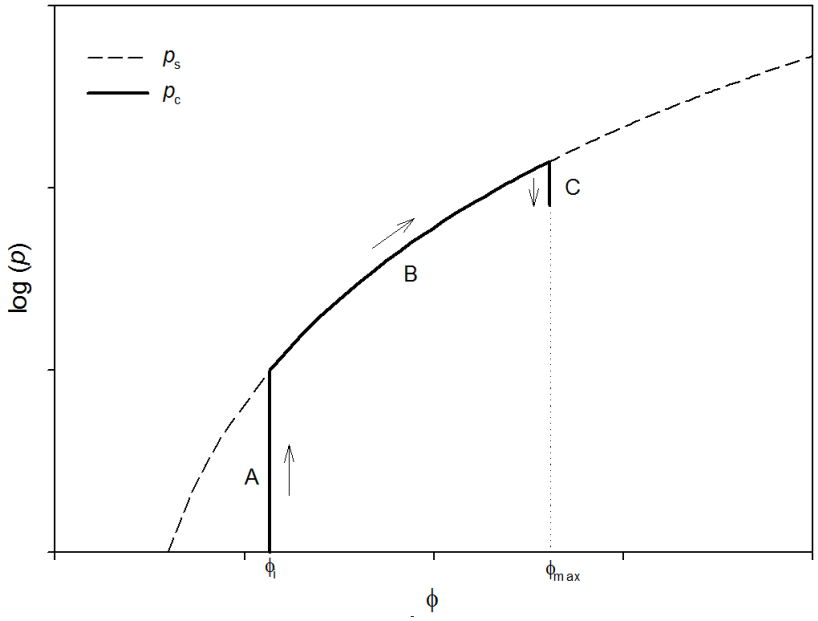

Fig. 2. Capillary pressure (P_c) during the drying of the sludge filter cake. The applied pressure (P_s) is shown as a function of the solid volume fraction.

When the thermogravimetric method is used to predict the maximum achievable dry matter content, the drying process is conducted slowly to ensure that the stress within the cake structure is equally distributed. It is implicitly assumed that the capillary pressure at the critical moisture point is comparable to the applied pressure used during mechanical dewatering, so the maximum dry matter content achievable by mechanical dewatering equals the critical moisture point. The relative humidity of the drying air affects the drying rate, but has only a minor influence on the critical moisture point (8).

The maximum achievable dry matter content depends on the sludge composition. A high concentration of organic materials reduces the dry matter content (1), so better degradation of the sludge during digestion usually improves the dewaterability. To obtain a more thorough understanding of the dewatering process, the concept of water pools has been introduced by dividing the water into free water and bound water (9–13). Unlike bound water, free water is unaffected by solid particles and capillary forces. Bound water has further been divided into three types of water: I) water trapped inside the crevices and interstitial space of the flocs (i.e., interstitial water), II) water physically bound to surfaces (i.e., vicinal water), and III) water chemically

bound to solid materials (i.e., water of hydration) (9). Various methods have been developed to quantify the different water pools in sludge and to distinguish between free and bound water, including dilatometry, centrifugal settling, filtration, differential scanning calorimetry, and nuclear magnetic resonance spectroscopy (9,12,14,15). The results depend on the chosen method, i.e., the selected measurement technique defines the amount of bound water (12), and there is no clear boundary between free and bound water (14). Furthermore, there are different explanations of the water content of dewatered sludge. High moisture content after dewatering has been explained as resulting from the colligative properties, i.e., the reduced water activity in the floc interior due to counterions (i.e., osmotic water) (16). Mikkelsen and Keiding (2002) used the term "water-holding" to refer to the surface-bound water, osmotic water, and trapped water (17), a concept also used for food products (18). It is argued that osmotic pressure increases at a lower moisture content because the concentration of counterions increases, reducing the dry matter content obtainable by mechanical dewatering (17). A method to study this "water-holding" is to measure the water activity. The water activity is defined as the ratio between the partial vapour pressure of water in a substance and the standard state partial vapour pressure of water. Water activity can be measured at different moisture contents (moisture vapour sorption curves) and used to study both water adsorption and "osmotic water" (8,19,20). Both adsorption and desorption isotherms have been determined for sludge, and almost no hysteresis has been observed (20). Moisture vapour sorption curves are routinely determined for food products (18). At low water activities ($a_w < 0.3$), the Langmuir sorption isotherm often gives fairly good predictions for food products (21). The Langmuir isotherm assumes the adsorption of a monolayer of water. The formation of a monolayer on solid materials corresponds to vicinal water and water of hydration. At higher water activities, the Guggenheim-Anderson-Boer (GAB) sorption isotherm has been used, as it includes both monolayer and multilayer sorption. The GAB sorption isotherm can often be used for water activities up to 0.95 (18,22). It is assumed that the sorption energy for water molecules in the layers beyond the monolayer is the same for all water molecules but different from that of the pure liquid state. An alternative to the GAB isotherm is the Blahovec and Yanniotis sorption isotherm, which includes the osmotic effect due to dissolved salts and counterions (23). The sorption isotherms include vicinal water, water of hydration, and osmotic water; trapped water or capillary water is not included in the three sorption models.

The aim of this study is to compare the thermogravimetric method and water sorption curves, thereby discussing how sludge composition and structure affect the water activity, critical moisture point, and dewaterability of sludge. The capillary effect and cake structure are included as part of the moisture vapour sorption isotherms. By doing this, the experimental data are used to discuss whether the water pool model or the osmotic pressure gives the best explanation of the critical moisture point, and of how the critical moisture point is related to the dry matter content after sludge dewatering.

2. Materials and methods

2.1. Sample

Digested sludge was obtained from Bruunshåb wastewater treatment plant (WWTP), which was loaded with approximately 45,000 population equivalents. Primary and secondary sludge was digested with a retention time of 2–4 days. After digestion, the sludge was coagulated with 1 L m^{-3} of 30–40% polyaluminium chloride (PAC) (PAX-215; Kemira, Helsinki, Finland) or 1.5 L m^{-3} of iron sulphate (PIX-113; Kemira). The coagulated sludge was flocculated (Aquaflok 71300BB) and dewatered using a screw press (Hjortkær Maskinfabrik, Årre, Denmark) to a dry matter content of 27% w/w. The raw digested sludge contained 40 ± 10 mg L^{-1} orthophosphate and 300 ± 100 mg L^{-1} chloride; the pH was measured to be 7.5 ± 1, and 60 ± 2% of the dry matter was organic materials.

An overview of the sampling points is given in Fig. 3. Untreated digested sludge (sample A), digested sludge with PAC (sample B1) or iron sulphate (sample B2), and dewatered digested sludge with iron sulphate and polymer (sample C) were sampled from the plant (Fig. 3). Further sodium chloride was added to untreated digested sludge to increase the conductivity from 9.22 mS cm^{-1} to 27.0 mS cm^{-1} (sample D).

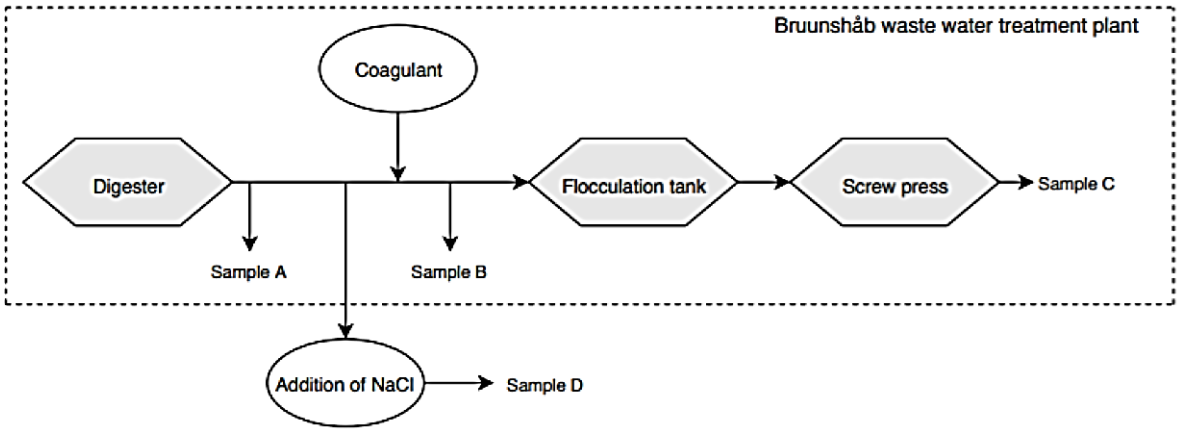

123

124 **Fig. 3.** Schematic of sampling points at the WWTP. NaCl was added to sample D after sampling.

125 The moisture content was estimated by leaving approximately 15 g of pre-weighed samples in an oven at
126 105°C for 24 h. The organic dry matter content was determined by incinerating the dried sample in the oven
127 at 550°C for 2 h. The organic matter was determined as the weight loss. The moisture content of the samples
128 is shown in Table 1.

129

130 *2.2. Thermogravimetric analysis*

131 Before thermogravimetric analysis, all samples were centrifuged at 1000 g for 30 min to lower the moisture
132 content (but still to a moisture content higher than the critical moisture point) and thereby the time required
133 for the drying process. The optical density of the supernatant was measured to be 550 nm.

134 Thermogravimetric analysis was conducted at both 27°C and 35.5°C using an Ova-Easy 190 cabinet
135 incubator (Brinsea Products, Titusville, FL, USA) and a humidity pump (Advance Humidity Pump; Brinsea).
136 A weighing scale was installed in the incubator and data were collected on-line by a computer. Multiple
137 small fans ensured laminar flow in the incubator. A Petri dish with an inner diameter of 50 mm was filled
138 with 16.2 g of wet sample (sludge A) and dried at 27.5°C, a relative humidity of 40 ± 5%, and an air flow of
139 0.5–1 m/s. The temperature at the surface was approximately 25°C, comparable to the temperature used for

140 the water activity measurements. The next experiments were conducted in 50-mm Petri dishes containing
141 approximately 15 g of wet samples (sludges A, B1, and B2), which were dried at 35.5°C. The temperature
142 was similar to that used by Kopp et al. (3). The temperature at the surface of the sludge cake was measured
143 to be 32°C. The average height of the samples was 13 mm before the drying process. For some of the
144 experiments, samples were taken every hour. These data indicate that the sample materials covered the Petri
145 dishes during the constant rate period but curled up during the falling rate period.

146 The critical moisture point was determined by plotting the drying rate as a function of the moisture point.
147 Linear regression was used to correlate the moisture content and the drying rate at high moisture contents (X
148 > 5 kg kg^{-1}). The critical moisture point was identified as the point at which the drying rate drops faster than
149 predicted by the regression line. The transition between the first and second falling rate periods was
150 determined by plotting the drying rate as a function of the logarithmic moisture point and identifying the
151 point at which the slope of the curve changes.

152 *2.3. Water activity*

153 The samples were taken before the screw press (samples A, B2, and D), and were centrifuged at 5000 g for
154 30 min to lower the moisture content before the water activity experiment. This reduced the required time to
155 reach equilibrium between water in the cake and in the air. Sample C was taken after the screw press and was
156 not centrifuged. The moisture content of the samples is shown in Table 1.

157

158 **Table 1**

159 Moisture content of sludge samples before and after centrifugation. Sample C was not centrifuged, and the
160 dry matter content of sample D was not measured.

Sample	Moisture content (kg water/kg dry matter)	Moisture content after centrifugation (kg water/kg dry matter)

A	41	7.3
B2	48	7.6
C	2.7	Not centrifuged
D	41	6.0

Sludge samples of 2–9 g were spread out in a rectangular sample holder with a surface area of approximately 32 cm^2. Each sample was then placed in a closed glass container separated from a saturated salt solution (Fig. 4). The inner diameter of the glass container was 10–11 cm, and the container was closed with a rubber ring. Saturated LiBr, LiCl, $CaCl_2$, NaBr, KI, NaCl, and $(NH_4)_2SO_4$ were used to control the humidity in the containers. The volume of the salt solution was approximately 0.15 L and extra salt was added to ensure a saturated salt solution. The containers were stored in a cupboard at a constant temperature of 25 ± 0.6°C. The temperature was monitored automatically during the experiment to control the temperature variation. For all samples, the moisture content decreased during the experiment and water desorbed from the sludge sample. The samples were weighed regularly until they did not lose further weight; it was then assumed that desorption had reach equilibrium, i.e., the water activity equalled the relative humidity of the air.

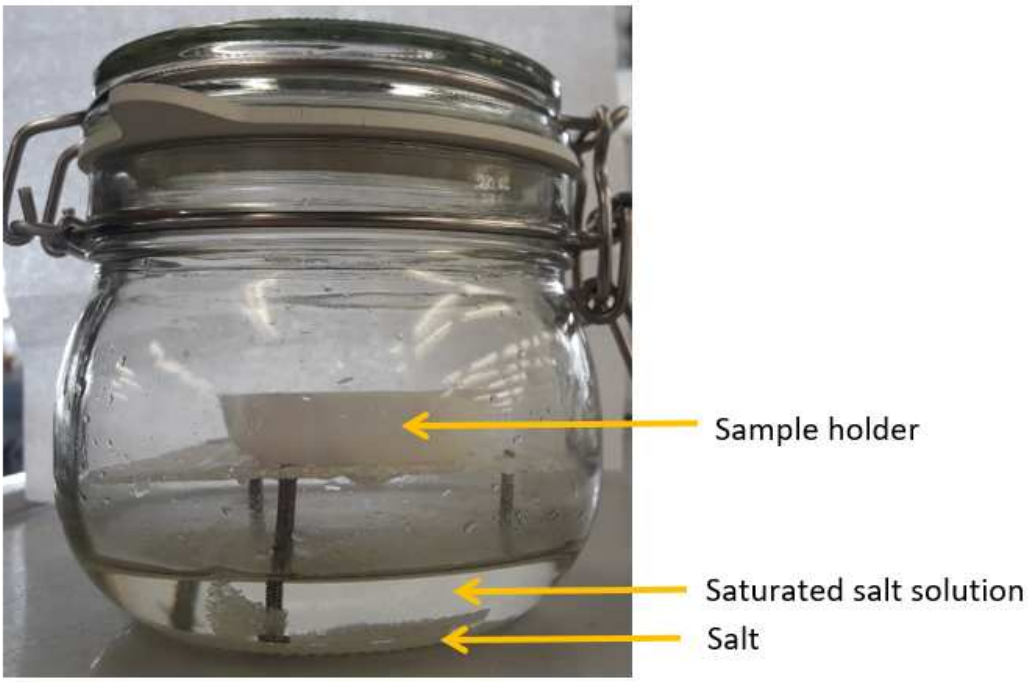

Fig. 4. Experimental setup for measuring water activity as a function of moisture content in sludge sample.

This was checked by measuring the water activity of the sludge sample and the salt solution using an Aqualab 4TE water activity meter (Meter Group, Pullman, WA, USA) at 25°C. After the experiment, the measured water activity was the same in the salt solution and the sludge sample (Fig. 5).

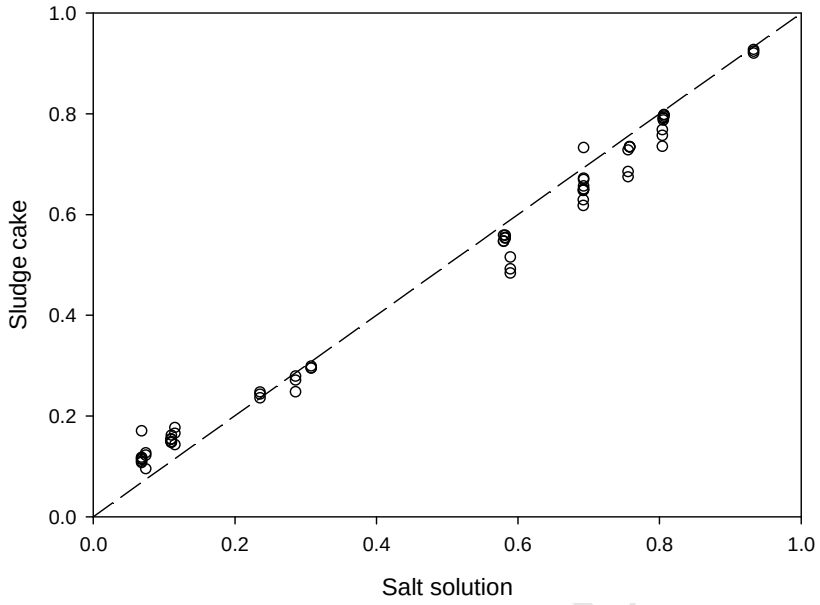

Fig. 5. Water activity measured in the salt solution and the sludge sample.

In the literature, almost no hysteresis has been observed in the sorption curves for sludge (20), so only desorption curves were measured. The weight of the wet and dry cake was measured by drying the cake at 105°C overnight, and the data were used to determine the moisture content. Samples were taken in triplicate. For all samples both water activity and moisture content were measured experimentally.

2.4. Water sorption isotherm

Three water sorption isotherms were fitted to the experimental data: Langmuir, Guggenheim-Anderson-Boer (GAB), and Blahovec and Yanniotis sorption isotherms.

187 The Langmuir sorption isotherm was used up to a water activity of 0.3, assuming the formation of a
188 monolayer of water:

189 $$X = \frac{X_{\mathrm{mL}} C_{\mathrm{L}} a_{\mathrm{w}}}{1 + C_{\mathrm{L}} a_w} \quad (1)$$

190 where X is the moisture content, X_{mL} the moisture content in a complete monolayer, C_{L} the equilibrium
191 constant, and a_{w} the water activity.

192 At higher water activities, multilayers of water were formed on the solid materials. The Guggenheim-
193 Anderson-Boer (GAB) sorption isotherm includes both mono- and multilayers. The GAB sorption isotherm
194 is a combination of the classical monolayer model expressed in the Langmuir isotherm and a multilayer
195 sorption term derived from Raoult's law (22). The parameter K was introduced, assuming that the multilayer
196 molecules interact with the solid materials and that the binding energy level ranges somewhere between
197 those of the monolayer molecules and the bulk liquid:

198 $$X = \frac{X_{\mathrm{mG}} C_{\mathrm{G}} a_{\mathrm{w}} K}{(1 - a_{\mathrm{w}} K)\,(1 + (C_{\mathrm{G}} - 1) a_w K)} \quad (2)$$

199 where X_{mG} is the moisture in a complete monolayer and C_{G} is the equilibrium constant. The value of C_{G} is
200 often a number between 1 and 20 (21). K captures the difference between the heat of adsorption and the heat
201 of vaporization of the multilayers, and its value ranges between 0.7 and 1 (21) . If K = 1, the GAB isotherm
202 is reduced to the BET isotherm.

203 The Blahovec and Yanniotis sorption isotherm includes the osmotic effect of salts and counterions (23). The
204 first part of the equation is the Langmuir isotherm and the last part a solution term accounting for the osmotic
205 effects:

206 $$X = \frac{a_{\mathrm{w}}}{a_1 + b_1 a_{\mathrm{w}}} + \frac{a_{\mathrm{w}}}{a_2 - b_2 a_{\mathrm{w}}} \quad (3)$$

207 and

208 $$a_1 = \frac{1}{C_B X_{mB}};\ b_1 = \frac{1}{X_{mB}};\ a_2 = \frac{\gamma}{M_w n_s};\ b_2 = \frac{1}{M_w n_s} \quad (4)$$

where X_{mB} is the moisture in a complete monolayer, C_B the equilibrium constant for monolayer adsorption, M_w the molecular weight of water, and n_s the molar amount of solute in solution per kg of dry matter. The solution term is derived from the non-ideal Raoult's law: $a_w = \gamma x_w$, where γ is the activity coefficient of water and x_w the mole fraction of water in solution.

All three isotherms were fitted to the experimental data using the least root mean square error method. The Langmuir sorption isotherm was fitted to the data up to a water activity of 0.3 by adjusting X_{mL} and C_L. These values were used as initial guesses for X_{mG} and C_G when the GAB sorption isotherm was used and for X_{xB} and C_B when the Blahovec and Yanniotis sorption isotherm was used. The GAB sorption isotherm was fitted to the experimental data up to a water activity of 0.95 by adjusting K, X_{mG}, and C_G. The Blahovec and Yanniotis sorption isotherm was fitted to the experimental data up to a water activity of 0.95 by adjusting n_s, X_{xB}, and C_B. The activity coefficient of water (γ) was set to 1 in the Blahovec and Yanniotis sorption isotherm. Some testing was done by adjusting n_s, X_{xB}, C_B, and γ; all resulted in γ values close to 1.

2.5. Pore radius estimation

The relationship between the moisture vapour pressure and surface curvature was calculated using the Kelvin equation, which for sphere-like pores takes the form:

$$RTln\left(\frac{p_0^k}{p_0}\right) = -\frac{2\gamma_L V_m}{r} \quad (5)$$

where p_0^k and p_0 are the vapour pressures for curved and flat surfaces, respectively. The vapour pressure for a flat surface equals $p_{0,w}\gamma x_w$, where $p_{0,w}$ is the vapour pressure for pure water and a flat surface. V_m is the molar volume of water, γ_L the surface tension of the liquid, and r the radius of the meniscus. For water, γ_L equals 72 mN m^{-1} at 25°C but decreases with pressure; for the salt solution, γ_L increases slightly.

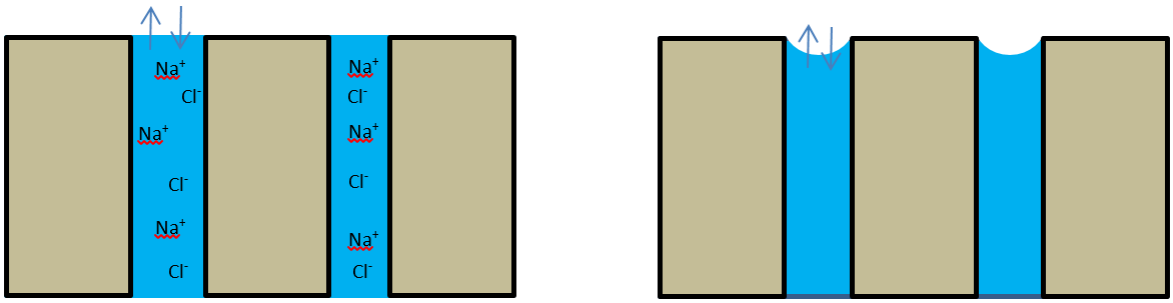

231

232 **Fig. 6.** Model of equilibrium between the liquid and gas phases at high moisture contents.

233 Two extreme cases were addressed in the paper (Fig. 6). In case 1, the equilibrium relative humidity was
234 assumed to equal the water activity determined by the salt concentration (flat surface, or $r \rightarrow \infty$ in Eq. 5), and
235 it was assumed that the water activity could be predicted by the GAB or the Blahovec and Yanniotis sorption
236 isotherm. In case 2, the relative humidity was assumed to be determined only by the capillary condensation.
237 It was assumed that the concentration of solutes was low, meaning that p_0 equalled the moisture vapour
238 pressure of pure water ($p_{0,w}$). Under these conditions, the measured water activity was not determined by the
239 non-ideal Raoult's law but by the curvature of the meniscus at the top of the sludge cake. By inserting a_w
240 into Eq. (5), the curvature of the meniscus was calculated as:

241 $$r = -\frac{2\gamma_L V_m}{RT \ln(a_w)} \quad (6)$$

242 The capillary pressure was calculated from the radius of the meniscus:

243 $$P_c = \frac{2(\gamma_S - \gamma_{SL})}{r} = \frac{2\gamma_L}{r}\cos\theta \approx \frac{2\gamma_L}{r} = -\frac{RT\ln(a_w)}{V_m} \quad (7)$$

244 where γ_S is the surface tension of the solid cake, γ_{SL} the interfacial tension between the cake and liquid, and
245 θ the contact angle. The contact angle is zero if the liquid spreads completely on the surface, meaning that
246 the capillary force can be calculated from the water activity. P_C is thereby calculated by using an equation
247 similar to the one used for calculating the osmotic pressure solutions.

248 During the constant rate period (Fig. 1), the curvature of the meniscus was determined by the strength of the
249 cake. The strength of the cake structure depends on the sludge composition and solid volume fraction. The
250 capillary pressure exceeds the pressure required to compress the cake structure (i.e., compressible yield
251 stress) during the constant rate period. Several empirical equations exist for calculating the solid volume
252 fraction as a function of pressure. Eq. (8) is often used for sludge (24):

253 $$\phi = \phi_0 \left(1 + \frac{P_s}{P_a}\right)^{\beta} \quad (8)$$

254 where ϕ is the solid volume fraction and p_s is the structural pressure, which equals the capillary pressure
255 during the constant rate period. Furthermore, ϕ_0 is the solid volume fraction at zero compression and P_a and
256 β are empirical parameters depending on the compressibility of the cake. Before the critical moisture point is
257 reached, the cake is wet and the moisture content (X) of the cake equals $(1 - \phi) \times \phi^{-1}$; after the critical
258 moisture point, air enters the cake and $X < (1 - \phi) \times \phi^{-1}$.

259 Setting Pc = Ps and combining Eqs. (7) and (8) gives:

260 $$\phi = \phi_0 \left(1 - \frac{RT \ln(a_w)}{V_m P_a}\right)^{\beta} \quad (9)$$

261 The capillary pressure at the critical moisture point was estimated from the measured water activity at the
262 critical moisture point using Eq. (7). The radius of the pores in the cake structure (r_c) was calculated from the
263 water activity at the critical moisture point (Eq. 6), at which the curvature of the meniscus equals the pore
264 size. Both calculations were undertaken assuming that the curvature at the surface determines the equilibrium
265 relative humidity (case 2). It may therefore be expected that the capillary pressure is overestimated and the
266 pore radius underestimated.

267

268 **3. Results and discussion**

The drying rate was constant for the first 10 h, after which it started to decline for digested sludge dried at 27.5°C (Fig. 7A). The drying rate was low due to the low temperature and high relative humidity. The critical moisture point was determined by plotting the drying rate as a function of the moisture content (Fig. 7B). The critical moisture point was determined to be 3.4 kg of water per kg of dry matter (23% w/w dry matter content). The transition between the first and second falling rate periods was more easily observed by plotting the drying rate as a function of the logarithmic moisture content (Fig. 7C). The moisture point at the transition was determined to be 0.59 kg of water per kg of dry matter. At the end of the drying process, the temperature at the surface increased to 27.5°C, the same temperature as the oven. The temperature started to increase during the second falling rate period.

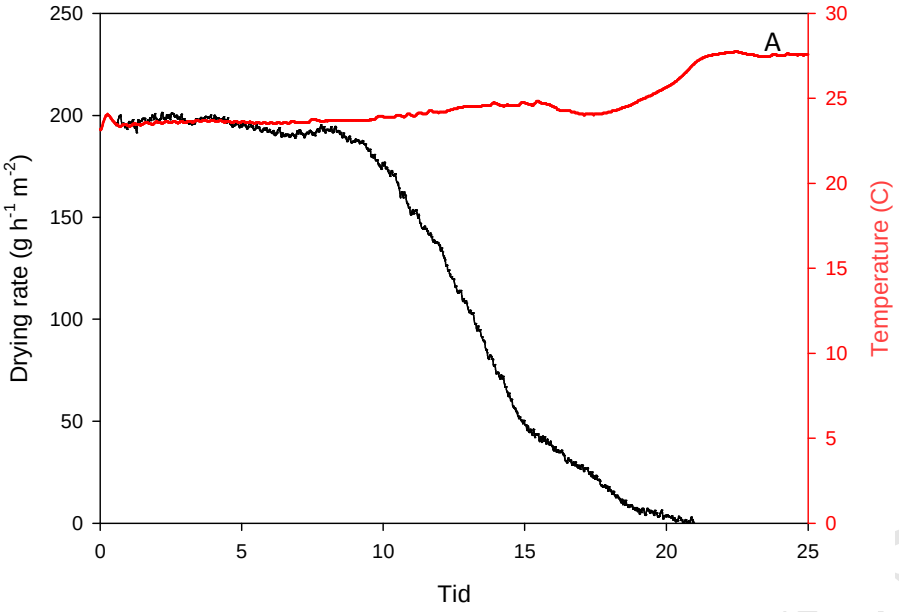
A
Drying rate (g h-1 m-2)
Temperature (C)
Tid
250
200
150
100
50
0
30
25
20
15
10
5
0
0
5
10
15
20
25

278

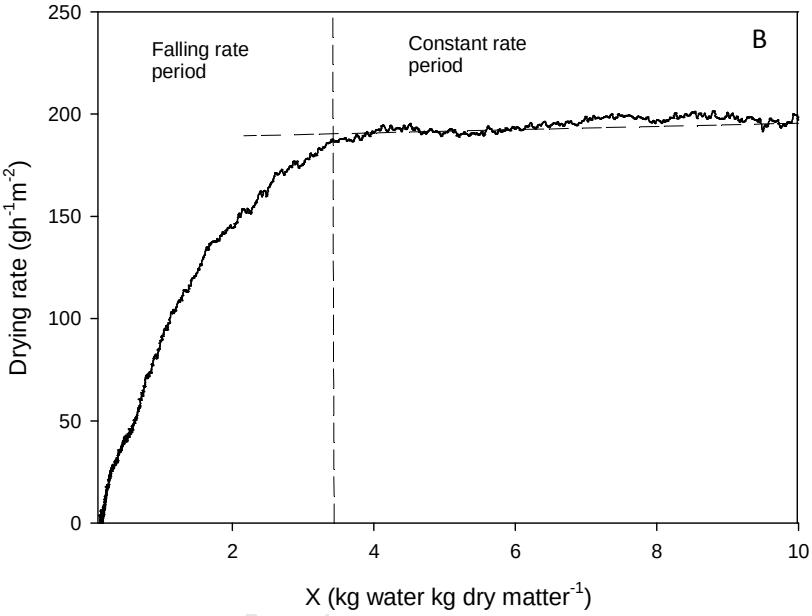
Falling rate period
Constant rate period
B
Drying rate (gh-1m-2)
X (kg water kg dry matter-1)
250
200
150
100
50
0
2
4
6
8
10

279

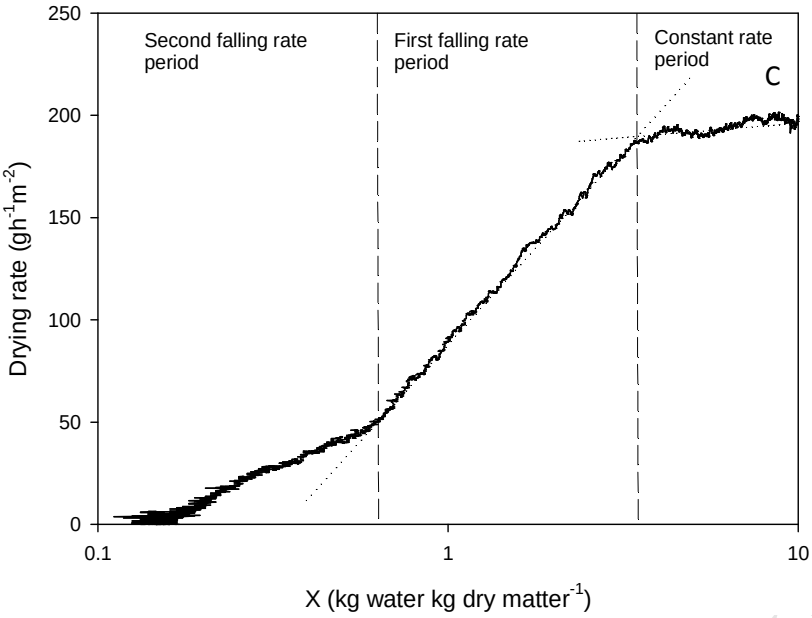

Fig. 7. (A) Drying curve for raw digested sludge (sludge A). Temperature is measured at the sludge surface. (B) Identification of the critical moisture point. (C) Identification of the critical moisture point and the transition from first to second falling rate periods.

Drying experiments were also conducted at 35.5°C; the drying curves from these experiments are shown in the supplementary material (Figs. S1–S3) and the key data in Table 2. The highest residual turbidity was obtained for raw sludge (sludge A). Both PAC and iron sulphate coagulants reduced the residual turbidity as expected when small particles were coagulated. PAC was most effective for reducing the residual turbidity. The drying rate declined for sludge B1 throughout the drying process, which may explain the lower moisture content at the critical moisture point. It may also be due to the higher drying rate, which increases the risk of crust formation (6,7). The drying rate was higher at 35.5°C than at 27.5°C, as expected, and higher for raw sludge than coagulated sludge. The critical moisture content was measured to be 3.4 kg of water per kg of dry matter. The critical moisture point was the same at both 27.5°C and 35.5°C, if data from sludge B1 (i.e., the coagulated sludge with a declining drying rate) were ignored. This may indicate that the determination of the critical moisture point is not sensitive to the drying temperature and rate if both these are low.

295 **Table 2**

296 Data for thermogravimetric analysis at 35.5°C.

	X_i	Organic fraction (%)	Turbidity	Max drying rate (gh^{-1} m^{-2})	X_c
Sludge A	10.4	37%	2.19	335	3.4
Sludge B1	12.3	36%	0.72	245	2.8
Sludge B2	10.9	38%	1.65	250	3.3

297

298 The moisture vapour sorption experiment was conducted for raw digested sludge (sludge A), conditioned
299 sludge (sludge B2), and dewatered sludge (sludge C). All adsorption curves follow the type II sigmoid shape
300 adsorption isotherm (18). Dewatering and the addition of coagulants and flocculants did not change the
301 moisture vapour sorption curve (Fig. 8A), whereas a high salt concentration affected the moisture vapour
302 sorption curve, but only for water activities higher than 0.6 (Fig. 8B). The Langmuir, GAB, and Blahovec
303 and Yanniotis sorption isotherms were fitted to the experimental data. The modelled data obtained with the
304 Langmuir and the Blahovec and Yanniotis sorption isotherms are shown in Figs. 8A and 8B. The modelled
305 data obtained using the GAB sorption isotherm are shown in the supplementary data (Figs. S4 and S5)

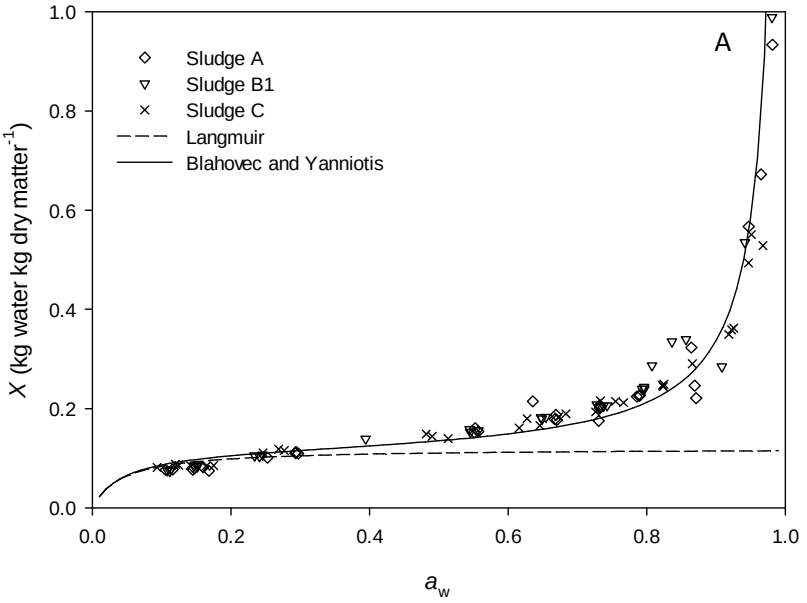

306

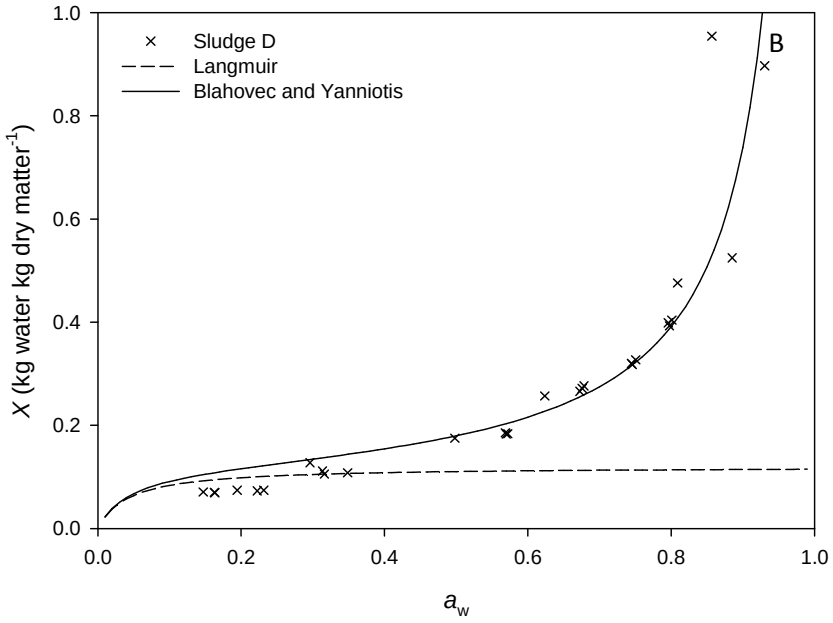

307

308 **Fig. 8.** (A) Water sorption isotherms for: digested sludge (Sludge A); conditioned digested sludges, one with
309 PAC (Sludge B1) and one with iron sulphate and polymer (Sludge D); and (B) Water sorption isotherm for
310 digested sludge with salt added (Sludge C).

All three sorption isotherms include a parameter for the maximum amount of water in a complete monolayer, i.e., 10–12 g per 100 g of dry matter (Table 2). Typical values for the moisture contents of monolayers for different food products are 3–19 g per 100 g of dry matter (18,25), and the amount of water in the complete monolayer was close to the value of, for example, gelatine (25). The value found for water in the monolayer was higher than that found by Vaxelaire et al. (2017), which was determined to be 7–8 g per 100 g of dry matter (19). The moisture content at the transition between the first and second falling rate periods was determined to be 59 g per 100 g of dry matter, corresponding to approximately five or six layers of water if the water was equally distributed within the cake. The water removed during the first falling rate period has been used as a measure of the interstitial water and the water removed during the second falling rate period as a measure of the surface water, i.e., the water adsorbed or adhering to the surfaces (13). However, no clear boundary was observed at the transition point on the moisture vapour sorption isotherms. The equilibrium constant C was calculated to be 22.9 when using the Langmuir and the Blahovec and Yanniotis isotherms and approximately 10 when using the GAB isotherm. The equilibrium constant was difficult to determine precisely, because an almost complete monolayer formed at the lowest water activity, and in another study the equilibrium constant was determined to be 60.5 (8). In the literature, the heat of adsorption has been measured at low moisture contents and found to decrease with the moisture content (13), indicating that the Langmuir isotherm assumption, i.e., that all surface sites are equivalent, is invalid. Still, the combined model including the Langmuir isotherm and both the GAB and the Blahovec and Yanniotis isotherms predicts a moisture content well above a water activity of 0.1.

The K value in the GAB sorption model was measured to be 0.8 for conditioned and raw sludges, similar to the value reported by Ruiz and Wisniewski (8), whereas the value was close to 1 for sludge with a high salt concentration. This indicates that the bonding becomes stronger when the salt concentration increases. The best fit was obtained using the Blahovec and Yanniotis sorption isotherm, indicating that the combination of the classical monolayer model expressed by the Langmuir isotherm and the water activity calculated from the ion concentration gives a fairly good description of water sorption. The osmotic effect increases the moisture content and may explain the different K values obtained before and after adding salt to the sludge.

Without salt addition, n_s was calculated to be 1.36 mmol per g of dry matter. The n_s value combines both the counterions and ions from the bulk solution. In other studies, the charge density for extracellular polymeric substances in sludge has been measured to be 0.2–1 mmol per g of EPS (16,17,26). Not all dry matter in sludge is EPS, so the total concentration of counterions is lower than 1 mmol per g of dry matter, but a large fraction of the ions seems to be counterions. When salt is added to the sludge, n_s increases as expected. At higher salt concentrations, the moisture content seems to be overestimated when using the Blahovec and Yannoitis sorption isotherm for low water activity, i.e., a_w 0.1–0.4. One possible reason for this overestimation is that ions precipitate at high concentrations, forming salt that does not contribute to the water activity at a low moisture content in the cake.

Table 3

Sorption isotherm constants.

	Parameter	Sludges A–C	Sludge D
Langmuir	X_{mL} (kg water/kg dry matter^{-1})	0.12	0.12
	C_L	22.9	22.9
GAB	X_{mG} (kg water/kg dry matter^{-1})	0.10	0.10
	C_G	13.3	8.58
	K	0.8	0.96
Blahovec and Yanniotis	X_{mB} (kg water/kg dry matter^{-1})	0.12	0.12
	C_B	22.9	22.9
	n_s (mol/kg dry matter)	1.36	3.54

At the critical moisture point, the moisture content is to some extent determined by the capillary effect and cake compressibility, which may be why the GAB and the Blahovec and Yanniotis sorption isotherms often do not predict the water activity well at water activities above 0.95. Furthermore, it is worth mentioning that precisely determining the water activity was difficult at high water activities. Nevertheless, if it is assumed

353 that the water activity experimentally measured from the relative humidity of the air is solely due to capillary
354 condensation, it is possible to estimate a value for the capillary pressure. The moisture content and water
355 activity are shown for water activities above 0.95 and moisture contents between 1 and 10 (Fig. 9). For the
356 sample with added salt (Sludge D), the moisture content is generally higher, which may reflect a tighter cake
357 structure, but the higher moisture content is probably due to the reduction of the water activity due to the
358 high concentration of ions. This shows that capillary condensation is not the only important parameter, at
359 least not for sludgeD.

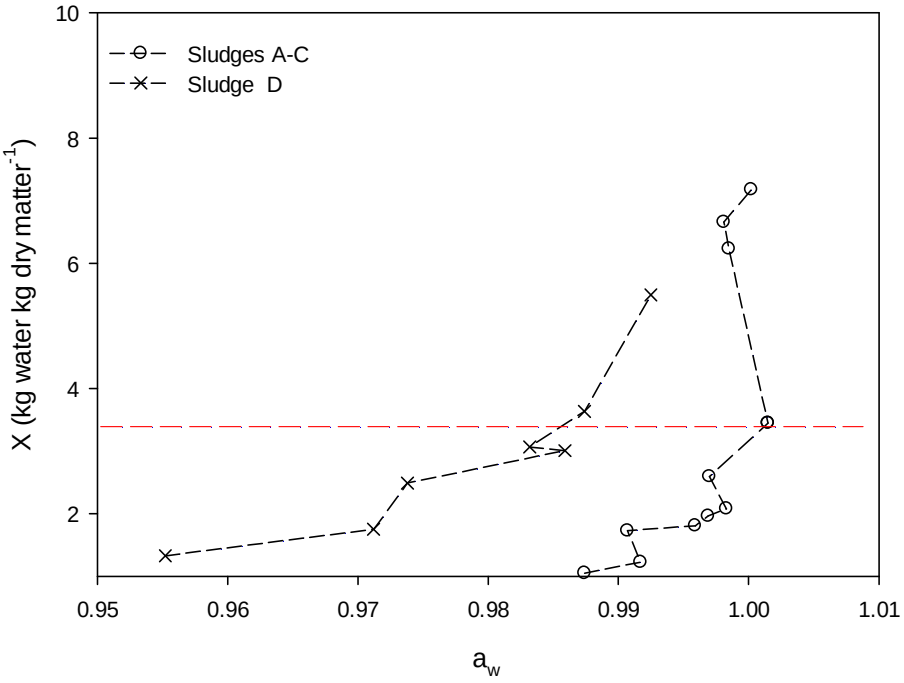

360

361 **Fig. 9.** Moisture content and water activity above a water activity of 1 (the dotted black lines are only to
362 guide the eyes). The dotted red line at a moisture content of 3.4 represents the measured critical moisture
363 content.

364 The capillary pressure for sludges A–C was calculated to be 4–6 bars and the radius of the pores was
365 estimated to be 200–300 nm. The moisture content of the dewatered cake was 2.7 kg of water per kg of dry
366 matter, i.e., 27% w/w dry matter content, which was 4 percentage points higher than that measured using the
367 thermogravimetric method at 25°C (Table 1). This may be due to the relatively low capillary pressure

368 compared with the applied pressure when the screw press was used. If ions affect the water activity, the
369 capillary pressure may even be lower. Using the value for n_s calculated from the Blahovec and Yanniotis
370 sorption isotherm results in an ion concentration of 0.4 M, which may have a significant impact on the water
371 activity. For sludge D, n_s was 3.85 mol per kg of dry matter, meaning that the ion concentration was
372 calculated to be 1 M at a moisture content of 3.4 kg of water per kg of dry matter. Comparing the data and
373 the two models of water distribution between sludge cake and air at a high moisture content indicates that the
374 cake structure is important for the relative humidity at equilibrium and thereby for the critical moisture point
375 (case 1, Fig. 6). Still, the salt content has a significant impact on the result. Thus, during the drying process,
376 the critical moisture point is a function of the pore size, cake compressibility, and salt content. The critical
377 moisture point is therefore determined by the cake compressibility, which also determines the dry matter
378 content during mechanical dewatering. Furthermore, cake compressibility is a measure of the dry matter
379 content as a function of applied pressure. The dry matter content increases at higher pressure; hence, if the
380 capillary pressure is high during the drying process, for example, due to small pores in the cake structure, the
381 value may be a relevant parameter for the maximum dry matter content obtainable during dewatering.
382 However, the estimated dry matter content is a function of the cake compressibility and capillary pressure.

383

384 **4. Conclusion**

385 The critical moisture point for digested sludge was determined thermogravimetrically to be 3.4 kg of water
386 per kg of dry matter. Data were compared with moisture vapour sorption isotherms. Conditioning and
387 dewatering did not affect the isotherms. Approximately 11 g of water adsorbs as a monolayer per 100 g of
388 dry matter. The rest of the sorption curve was well explained by the non-ideal Raoul's law by including the
389 effects of dissolved ions. The Blahovec and Yanniotis sorption isotherm fit the data well up to a water
390 activity of approximately 0.95. At water activities above 0.95, the moisture content was affected by the
391 meniscus at the cake surface and by the cake compressibility, but dissolved ions still played a role. The
392 critical moisture point was a function of the ion concentration, pore size, and cake compressibility. Thus, the

393 critical moisture point may only be a good estimate of the maximum dry matter content achievable by
394 dewatering if the capillary pressure at the moisture point is comparable to the structural pressure obtained
395 during mechanical dewatering.

396

397 **5. Acknowledgements**

398 DANVA is gratefully acknowledged for funding the VUDP project "Rethink sludge – optimering af
399 slamafvandingen via online sensorer kombineret med kamerateknologi", ID no. 1170.2017. The authors
400 thank Mogens Lindgaard from Centralrenseanlægget i Bruunshåb for his help with sampling and handling
401 the sludge.

402

403 **References**

404 1. Kopp J, Dichtl N. Prediction of full-scale dewatering results by determining the water distribution of
405 sewage sludges. Water Sci Technol. 2000;42(9):141–9.

406 2. Kopp J, Dichtl N. Prediction of full-scale dewatering results of sewage sludges by the physical water
407 distribution. Water Sci Technol. 2001;43(11):135–43.

408 3. Kopp J, Dichtl N. Influence of the free water content on the dewaterability of sewage sludges. Water
409 Sci Technol. 2001;44(10):177–83.

410 4. Scherer GW. Theory of Drying. J Am Ceram Soc. 1990;73(1):3–14.

411 5. Bennamoun L, Arlabosse P, Léonard A. Review on fundamental aspect of application of drying
412 process to wastewater sludge. Renew Sustain Energy Rev. 2013;28:29–43.

413 6. Vaxelaire J, Bongiovanni JM, Mousques P, Puiggali JR. Thermal drying of residual sludge. Water
414 Res. 2000;

7. Léonard A, Blacher S, Marchot P, Pirard JP, Crine M. Convective drying of wastewater sludges: Influence of air temperature, superficial velocity, and humidity on the kinetics. Dry Technol. 2005;

8. Ruiz T, Wisniewski C. Correlation between dewatering and hydro-textural characteristics of sewage sludge during drying. Sep Purif Technol. 2008;61:204–10.

9. Vesilind PA. The role of water in sludge dewatering. Water Environ Res. 1994;66(1):4–11.

10. Smith JK, Vesilind PA. Dilatometric measurement of bound water in wastewater sludge. Water Res. 1995;29(12):2621–6.

11. Vesilind PA, Martel CJ. Freezing of Water and Wastewater Sludges. J Environ Eng. 2007;116(5):854–62.

12. Vaxelaire J, Cézac P. Moisture distribution in activated sludges: A review. Water Res. 2004;38(9):2214–29.

13. Deng W, Li X, Yan J, Wang F, Chi Y, Cen K. Moisture distribution in sludges based on different testing methods. J Environ Sci. 2011;23(5):875–80.

14. Wu B, Zhou K, He Y, Chai X, Dai X. Unraveling the water states of waste-activated sludge through transverse spin-spin relaxation time of low-field NMR. Water Res. 2019;155:266–74.

15. He DQ, Zhang YJ, He CS, Yu HQ. Changing profiles of bound water content and distribution in the activated sludge treatment by NaCl addition and pH modification. Chemosphere. 2017;186:702–8.

16. Keiding K, Wybrandt L, Nielsen PH. Remember the water - A comment on EPS colligative properties. Water Sci Technol. 2001;43(6):17–23.

17. Mikkelsen LH, Keiding K. Physico-chemical characteristics of full scale sewage sludges with implications to dewatering. Water Res. 2002;36(10):2451–62.

18. Al-Muhtaseb AH, McMinn WAM, Magee TRA. Moisture sorption isotherm characteristics of food

products: A review. Food Bioprod Process Trans Inst Chem Eng Part C. 2002;80:118–28.

19. Vaxelaire J, Mousques P, Bongiovanni JM, Puiggali JR. Desorption isotherms of domestic activated sludge. Environ Technol (United Kingdom). 2000;21(3):327–35.

20. Bougayr EH, Lakhal EK, Idlimam A, Lamharrar A, Kouhila M, Berroug F. Experimental study of hygroscopic equilibrium and thermodynamic properties of sewage sludge. Appl Therm Eng. 2018;143:521–31.

21. Barbosa-Canovas G V. Water activity in foods : fundamentals and applications. Elektronis. Barbosa-Canovas G V, editor. Palo Alto, Calif. : ebrary; 2007.

22. Basu S, Shivhare US, Mujumdar AS. Models for sorption isotherms for foods: A review. Dry Technol. 2006;24(8):917–30.

23. Blahovec J, Yanniotis S. Modified classification of sorption isotherms. J Food Eng. 2009;91(1):72–7.

24. Tiller FM, Leu W-F. Basic data fitting in filtration. J Chin Inst Chem Eng. 1980;11(2):61–70.

25. Labuza TP, Altunakar B. Water Activity Prediction and Moisture Sorption Isotherms. In: Water Activity in Foods: Fundamentals and Applications. 2008.

26. Raynaud M, Vaxelaire J, Olivier J, Dieudé-Fauvel E, Baudez JC. Compression dewatering of municipal activated sludge: Effects of salt and pH. Water Res. 2012;46(14):4448–56.

Highlights

Thermogravimetric analysis and vapor sorption measurements was done for digested sludge

Blahovec and Yanniotis sorption isotherm fit vapor sorption curves well up to water activities of 0.95

Above water activities of 0.95 capillary condensations dominates

Cake compression and capillary pressure determined the critical moisture point

The capillary pressure was estimated to be 4-6 bars at the critical moisture point